ChemPubSoc Europe

DOI: 10.1002/chem.201402923

CHEMISTRY
A European Journal
Full Paper

Coordination Polymers

Controlled Synthesis of Porous Coordination-Polymer Microcrystals with Definite Morphologies and Sizes under Mild Conditions

Qing Liu, Ji-Min Yang, Li-Na Jin, and Wei-Yin Sun*[a]

Abstract: Herein, we report a facile and convenient method for the synthesis of the porous coordination polymer MOF-14 [$Cu_3(BTB)_2$] (H_3BTB = 4,4′,4″-benzene-1,3,5-triyl-tribenzoic acid) as microcrystals with definite shapes and crystal facets controlled by the reaction medium at room temperature. The amount of sodium acetate added to the reaction system plays a crucial role in the shape evolution of MOF-14 from rhombic dodecahedrons to truncated rhombic dodecahedrons and cubes with truncated edges and then to cubes. The addition of a base could accelerate the formation rate of crystal growth and increase the supersaturation of crystal growth, thus resulting in the formation of MOF-14 cube crystals with high-energy crystal facets. The morphological evolution was also observed for HKUST-1 [$Cu_3(BTC)_2$] (H_3BTC = 1,3,5-benzenetricarbocylic acid) from octahedrons to cubes, thus verifying the probable mechanism of the morphological transformation. The gas-adsorption properties of MOF-14 with different shapes were studied and reveal that the porous coordination-polymer microcrystals display excellent and morphology-dependent sorption properties.

Introduction

Over the past decade, crystals with specific morphologies and sizes have attracted great interest from researchers because the physical and chemical properties of crystals are intensively determined not only by their chemical composition, but also by the morphology, size,[1] and the exposed facets of the crystals.[2] For example, noble-metal nanocrystals with high-energy facets generally show much higher catalytic activity than such crystals with low-energy facets.[3] Therefore, the controlled synthesis of crystals with specific crystal facets is desired, but still a challenge.

Porous coordination polymers (PCPs) or metal–organic frameworks (MOFs), which are considered as a unique class of inorganic–organic hybrid material with metal centers and organic linkers,[4] have received growing attention in recent years because of their tailored pore structure; high surface area; interesting properties, such as gas adsorption; and potential use in storage,[5] drug release,[6] sensing,[7] membranes,[8] and catalysis.[9] In addition, relative to the bulk MOFs materials, nanosized MOF (NMOF) materials have become increasingly interesting because their nano-/microstructure, morphology, size, and crystal facets play an important role in determining the property and application of NMOFs materials.[10] Therefore, controlled synthesis of well-defined NMOFs crystals with definite morphology, size, and specific exposed crystal facets is highly desirable. However, it is still difficult to develop a facile synthetic method to achieve such a target due to the variety in MOFs structures and various factors that affect the crystal shape and size.

To date, several strategies have been employed to fabricate NMOFs, such as direct precipitation,[11] hydro-/solvothermal techniques,[10b,12] and microwave-assisted,[13] sonochemical, and electrochemical syntheses.[14] Among these approaches, direct precipitation at room temperature, in which solutions of metal salts and organic linkers are mixed directly, is the simplest method to produce NMOFs. On the other hand, the use of various additives is an important synthetic approach to the fabrication of NMOF materials with tunable morphologies and sizes because the additives can affect the nucleation and growth process of NMOFs. Coordination modulators, such as monocarboxylic acids and their salts, have been widely used as the additives or capping agents for the preparation of NMOFs, which can alter the coordination equilibrium at the crystal surface during the nucleation and growth process.[13,15] Kitagawa and co-workers used the combination of coordination modulation and microwave synthesis to control the size and morphology of HKUST-1 [$Cu_3(BTC)_2$] (H_3BTC = 1,3,5-benzenetricarbocylic acid), in which dodecanoic acid was employed as the coordination modulator.[13] Fischer and co-workers obtained stable and size-selected MOF-5 colloids by the addition of *para*-perfluoroethylbenzoic acid as a capping reagent.[15] Furthermore, N-heterocyclic compounds and alkylamines were also used as coordination modulators in the synthesis of MOFs.[16,17] Oh and

[a] Q. Liu, J.-M. Yang, Dr. L.-N. Jin, Prof. Dr. W.-Y. Sun
State Key Laboratory of Coordination Chemistry
Coordination Chemistry Institute
School of Chemistry and Chemical Engineering
Nanjing National Laboratory of Microstructures
Nanjing University, Nanjing 210093 (P.R. China)
Fax: (+86) 25-83314502
E-mail: sunwy@nju.edu.cn

Supporting information for this article is available on the WWW under http://dx.doi.org/10.1002/chem.201402923.

co-workers reported that the addition of pyridine in the solvothermal synthesis of In-MIL-53 [In(OH)(BDC)] (H_2BDC = 1,4-benzenedicarboxylic acid) could manipulate the morphology of the microsized crystals.[16] Huber and Wiebcke reported a rapid room-temperature production of ZIF-8 (ZIF = zeolitic imidazolate framework) crystals of different sizes by employing an excess of auxiliary ligands, such as 1-methylimidazole and *n*-butylamine.[17] In addition, other kinds of additive, including surfactants and polymers, also have been used to control the morphology and size of NMOFs, which could suppress the growth of specific crystal facets.[11a,18,19] Our previously reported HKUST-1 crystals with a controllable morphology from cubes to octahedrons have been readily synthesized at room temperature by adjusting the concentration of cetyltrimethylammonium bromide (CTAB).[11a] Eddaoudi and co-workers reported that highly monodisperse M^{III}-soc-MOFs (M^{III}-based square-octahedral metal − organic frameworks, M = In and Ga) with a morphological evolution from simple cubes to complex octadecahedra were achieved by using a series of surfactants and structure-directing agents.[18] The porous coordination polymer $[Cu_2(PZDC)_2(PYZ)]$ ($PZDC^{2-}$ = pyrazine-2,3-dicarboxylate, PYZ = pyrazine) crystals with tunable sizes were prepared in a predictable manner by the addition of the organic polymer poly(vinylsulfonic acid) as a sodium salt.[19] However, an investigation of other types of additive, such as acids or bases, to control the morphology and size of NMOFs, especially by inducing the crystal-morphological evolution of polyhedrons with specific crystal facets, has not been realized so far to the best of our knowledge. Although it is known that the pH value of the reaction mixture can affect the nucleation rate, thus, controlling the particle size as a consequence, detailed studies on the morphological evolution of NMOFs crystals are rare.[20]

Herein, we report a simple and straightforward method for the morphology-controlled synthesis of porous coordination polymers by using different bases, such as sodium acetate, aqueous ammonia, triethylamine, and NaOH, in an aqueous solution with ethanol at room temperature. We chose the previously reported porous coordination polymers MOF-14 $[Cu_3(BTB)_2]$ (H_3BTB = 4,4′,4″-benzene-1,3,5-triyltribenzoic acid) and HKUST-1 as the candidate materials because they have dicopper paddle-wheel secondary building units, unsaturated metal centers upon activation, high porosity, and large specific surface areas.[21] The gas-adsorption properties of MOF-14 with different shapes were studied.

Results and Discussion

In contrast to the solvothermal and mechanochemical synthetic methods reported previously,[21,22] a facile and convenient method for the synthesis of MOF-14 was developed in this study. MOF-14 microcrystals were obtained through a solution approach at room temperature by using sodium acetate as an additive. The molar ratio of sodium acetate/H_3BTB plays an important role in determining the shape and size of the MOF-14 polyhedral microcrystals. In the absence of sodium acetate, the mixed solution of H_3BTB and $Cu(NO_3)_2{\cdot}3H_2O$ remained transparent for a few minutes and then a blue precipitate formed gradually; however, the products of the blue precipitate appeared immediately when sodium acetate was added into the reaction solution, thus implying that sodium acetate significantly accelerates the rate of formation of the products.

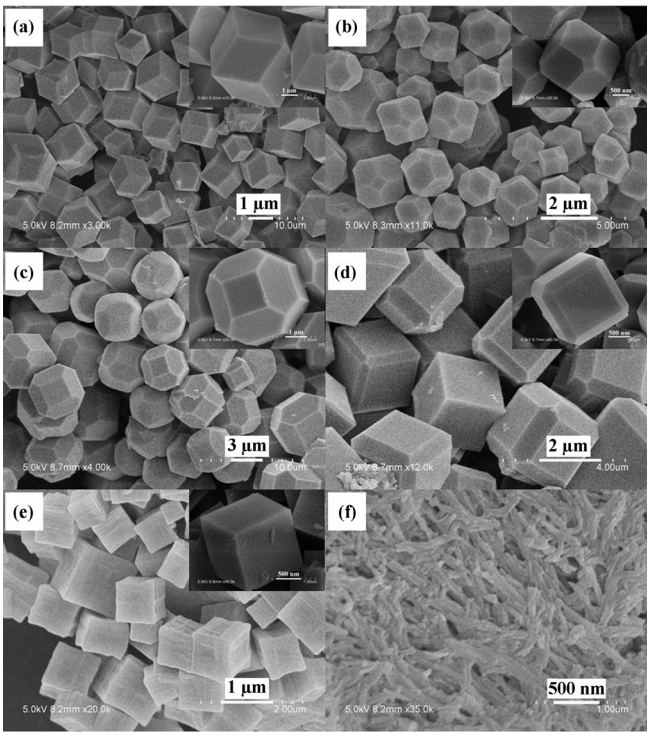

Figure 1. SEM images and high-magnification SEM images (inset) of MOF-14 microcrystals prepared with different amounts of sodium acetate: a) 0, b) 1, c) 2, d) 3, e) 4, and f) 5 equivalents.

Figure 1 shows the SEM images of the samples obtained with different amounts of sodium acetate. The crystals prepared without the addition of sodium acetate are rhombic dodecahedrons and the mean particle size is about 3–5 μm (Figure 1 a). When one equivalent of sodium acetate (given below as equivalents with respect to H_3BTB) was added, truncated rhombic dodecahedral crystals with average sizes of 2–3 μm were observed as illustrated in Figure 1 b. Two equivalents of sodium acetate also resulted in the formation of truncated rhombic dodecahedral crystals; however, the squares on the crystal surface became larger (Figure 1 c). The particle morphology changed to cubes with truncated edges with average sizes of 2 μm in the presence of three equivalents of sodium acetate (Figure 1 d). Figure 1 e shows that four equivalents of sodium acetate leads to the formation of cubic crystals, and the particle size is about 1 μm. When the amount of sodium acetate was further increased to five equivalents, rodlike crystals with narrow diameter distributions of approximately 1 μm in length and 100 nm in width were achieved (Figure 1 f). Obviously, with the amount of sodium acetate increased, an evolution of particle morphology from rhombic dodecahedron, truncated rhombic dodecahedron, and cube with truncated edges to cube was observed. Meanwhile, the particle size decreased gradually.

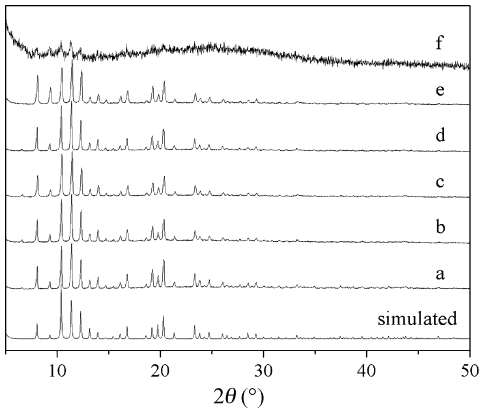

Figure 2. PXRD patterns of MOF-14 microcrystals prepared with different amounts of sodium acetate: a) 0, b) 1, c) 2, d) 3, e) 4, and f) 5 equivalents.

The structures of the samples prepared with different amount of sodium acetate were studied by powder X-ray diffraction (PXRD). All the characteristic diffraction peaks of MOF-14 were identified, and all the samples were pure-phase MOF-14 (Figure 2). The absence of sodium acetate in the products was further confirmed by elemental analysis (see the experimental details in the Supporting Information). Remarkably, when five equivalents of sodium acetate were added, all the characteristic diffraction peaks became very weak and the sample became amorphous. The above results indicate that the addition of sodium acetate not only accelerates the formation rate and affects the particle morphology and size of MOF-14, but also affects the structure of MOF-14.

FTIR spectroscopic data were used to characterize the obtained MOF-14 samples, which further support the chemical composition of the products (see Figure S1 in the Supporting Information). All the samples show similar characteristic bands in their IR spectra. The characteristic bands at $\tilde{\nu}=1585$ and 1401 cm^{-1} belong to the stretching vibrations of ν_{as}(–COO^-) and ν_s(–COO^-) of the carboxylate group of the BTB^{3-} ion, respectively, thus indicating that the carboxylate groups of the ligand are coordinated to the Cu^{II} center. In addition, the broad band at around $\tilde{\nu}=3420$ cm^{-1} indicates the presence of water molecules. The absence of characteristic bands of free H_3BTB at $\tilde{\nu}=1611$ and 1283 cm^{-1}, which belong to the stretching vibration of the C=O and C–OH groups, respectively, indicates that H_3BTB is completely deprotonated in MOF-14.

Typical thermogravimetric analysis (TGA) curves of MOF-14 microcrystals with different morphologies show that all the samples have similar weight-loss processes (see Figure S2 in the Supporting Information). The TGA curves recorded in N_2 exhibit two major weight losses in the temperature range 30–500 °C. The first weight loss below 200 °C is due to the elimination of solvent molecules. All the samples were stable up to 250 °C, in agreement with the reported stability of the bulk crystal sample.[21] When the temperature was above 300 °C, weight loss was observed, which is attributed to the decomposition of the framework. TGA results show that the microcrystal samples are as stable as the bulk samples and are not affected by the particle morphology greatly.

It is known that sodium acetate is not only a base that can deprotonate the H_3BTB ligand to accelerate the rate of formation of the products, but the acetate ion is a good coordination modulator that affects the nucleation and growth process of NMOFs. Acetic acid, which is considered as a good capping agent in the coordination modulation method, was initially chosen in the reaction system to explore the role of sodium acetate during the nucleation and growth process of MOF-14. When 1–4 equivalents of acetic acid with respect to the H_3BTB was added, the MOF-14 structures were not affected and the crystal morphology was rhombic dodecahedron (see Figures S3 and S4 in the Supporting Information), thus implying that the coordination role of the acetate ion does not work on the morphology of MOF-14 and the acid/base environment of the synthetic medium may determine the microcrystal morphology. A set of experiments was performed subsequently by using other kinds of base, including aqueous ammonia, triethylamine, and NaOH to verify this assumption. The particle morphology transforms from truncated rhombic dodecahedron to cube with the addition of 1–3 equivalents of ammonia (Figure 3a–c). When 1–3 equivalents of triethylamine was added,

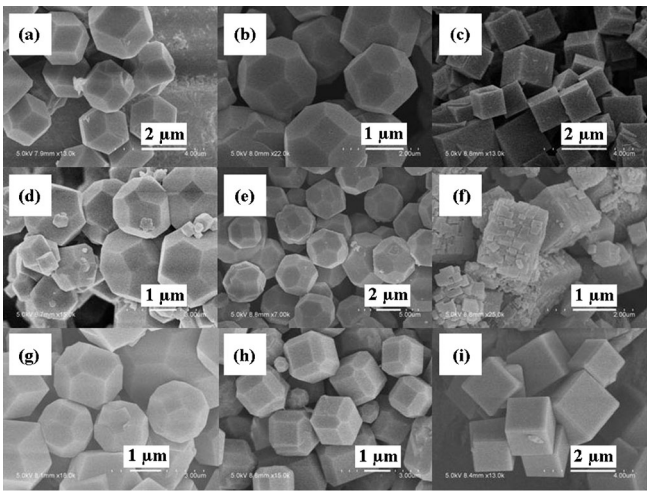

Figure 3. SEM images of MOF-14 microcrystals prepared with different amounts of ammonia: a) 1, b) 2, and c) 3 equivalents; triethylamine: d) 1, e) 2, and f) 3 equivalents; and NaOH: g) 1, h) 2, and i) 3 equivalents.

truncated rhombic dodecahedrons and cubes were obtained successively (Figure 3d–f). These two kinds of base that contain nitrogen atoms may affect the coordination equilibrium during the nucleation and growth process of MOF-14; therefore, the inorganic base NaOH was used to further verify our assumption. Truncated rhombic dodecahedrons, cubes with truncated edges, and cubes were observed by the addition of 1–3 equivalents of NaOH to the reaction (Figure 3 g –i). According to these observations, the morphology-evolution process of MOF-14 from rhombic dodecahedron to truncated rhombic dodecahedron and then to cube can be achieved only dependent on the amount of base, thus indicating that the crystal morphology is actually determined by the acid/base environment of the reaction.

To demonstrate further that this synthetic strategy is general, sodium acetate and other bases were utilized to prepare other NMOFs. HKUST-1,[23] which contains the benzenetricarboxylate ligand and possesses the same dicopper paddle-wheel secondary building units, was selected as an example. HKUST-1 was synthesized by mixing $Cu(NO_3)_2 \cdot 3H_2O$ and H_3BTC in a 1:1 (v/v) mixed solvent of ethanol and deionized water at room temperature with different amounts of sodium acetate and confirmed by means of PXRD measurements (see Figure S5 in the Supporting Information).

In the absence of sodium acetate, irregularly octahedral microcrystals were obtained by stirring at room temperature (Figure 4a). When one equivalent of sodium acetate with respect to H_3BTC was added to the reaction mixture, the particle morphology also was octahedron as shown in Figure 4b. On increasing the amount of sodium acetate to two equivalents, irregular truncated octahedrons and cuboctahedrons were observed (Figure 4c). When three equivalents of sodium acetate with respect to H_3BTC was added, the particles have cuboctahedral shapes (Figure 4d). A further addition of four equivalents of sodium acetate with respect to H_3BTC in the reaction mixture meant that the crystal morphology changed to truncated cube or cube (Figure 4e). At the same time, the particle size decreased from 2–3 μm to 500 nm with increasing amounts of sodium acetate. When other bases, such as aqueous ammonia and NaOH, were employed, the particle morphology also transformed from octahedron to cuboctahedron and finally to cube (see Figures S6 and S7 in the Supporting Information). The morphological evaluation of HKUST-1 was also only affected by the amount of base, thus implying that the particle shapes of porous coordination polymers can be determined by the acid/base environment of the reaction medium. On the basis of these results, it can be concluded that the shape-controlled synthesis of porous coordination polymers can be achieved by adjusting the acid/base environment of the reaction at room temperature in a mixed solvent of ethanol and water.

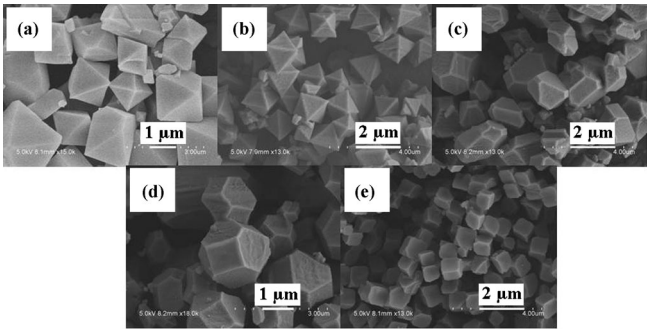

Figure 4. SEM images of HKUST-1 microcrystals prepared with different amounts of sodium acetate: a) 0, b) 1, c) 2, d) 3, and e) 4 equivalents.

It is known that the morphology of crystals is mainly determined by the surface energy of the crystal facets and the crystallite enclosed by crystallographic facets with the lowest surface energy is the most stable structure and readily formed under ordinary conditions. At the same time, it has been proposed that the supersaturation of crystal-growth units during the crystal-growth process could affect the surface energy, thus controlling the shape and surface structures of the crystals. The crystal faces with higher surface energy will be observed with increased supersaturation of the growth units.[24] In this study, the XRD diffraction peaks of MOF-14 can be indexed as a body-centered cubic (bcc) structure ($a=b=c=$ 26.496 Å, $\alpha=\beta=\gamma=90^\circ$, space group $Im\bar{3}$), thus indicating that MOF-14 adopts the bcc structure and the {110} surfaces have the lowest surface energy, whereas the surface energy of the {100} surface is higher than that of the {110} surface.[24] Therefore, rhombic dodecahedral crystallites with 12×{110} faces, which have the lowest surface energy and the most stable structure, could be obtained with stirring without any additives at room temperature. When sodium acetate was added to the reaction system, the ligand H_3BTB was deprotonated, and coordinates with the Cu^{II} center quickly, thus accelerating the formation of the crystal-growth units and yielding a high supersaturation of crystal-growth units in the reaction system. As a result, crystal facets {100} with higher surface energy are formed. On increasing the amount of sodium acetate, supersaturation of the crystal-growth units also increases and the area of crystal facets {100} get larger on the crystal surface. Therefore, truncated rhombic dodecahedrons and cubes with truncated edges, which consist of {110} and {100} facets, are obtained in succession. When the molar ratio of sodium acetate/H_3BTB was high enough, which causes higher supersaturation of the crystal-growth units, the low-energy surfaces {110} totally disappeared, and MOF-14 cube crystals with six high-energy surfaces {100} were finally achieved. In conclusion, the addition of sodium acetate to the reaction system could accelerate the formation rate of crystal-growth units and increase the supersaturation, thus resulting in the formation of cubic MOF-14 crystallites with crystal faces of a higher surface energy (Figure 5).

The formation of HKUST-1 with different morphologies can also be explained by the above surface-energy-driven mecha-

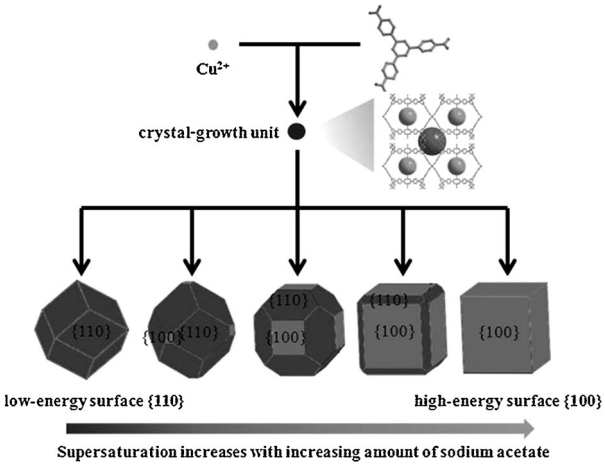

Figure 5. A schematic illustration of the shape evolution of MOF-14 microcrystals with varied morphologies.

nism (see Figure S8 in the Supporting Information). The crystal structure of HKUST-1 (space group $Fm\bar{3}m$) can be represented as a face-centered cubic (fcc) structure, in which the surface energy of the {111} facets is the lowest and the surface energy of the {100} surfaces is higher than that of the {111} facet.[25] Octahedral HKUST-1 crystallites with 8×{111} surfaces are the most stable structure and are formed without any additives under mild conditions. With the addition of sodium acetate to the reaction mixture, the deprotonation rate of H_3BTC accelerates and the crystal-growth units are rapidly yielded, thus resulting in higher supersaturation. Therefore, high-energy surfaces {100} appear and the particle shape of HKUST-1 changes from octahedron to cuboctahedron (enclosed by 8×{111} and 6×{100} faces) and then cube (enclosed by 6×{100} faces). The above discussion can explain the crystal-formation mechanism and the role of the base in the reaction process. The addition of the base accelerates the deprotonation rate of the carboxylic acid ligands and the reaction rate for the formation of porous coordination polymers, thus increasing the supersaturation of crystal-growth units and resulting in crystals with specific crystal facets.

The solvent is another important factor that affects the particle morphology and size in the synthesis of MOFs, and the volume ratio of ethanol/water plays a crucial role in the formation of MOF-14 of different morphologies. When the solvent consists of 20 mL of 1:1 mixture of ethanol and water, individual spherelike superstructures accumulated by numerous polyhedral units were observed (see Figure S9a in the Supporting Information). On the addition of one equivalent of sodium acetate with respect to H_3BTB, irregular microspheres with rough surfaces were obtained (see Figure S9b in the Supporting Information). Amorphous beltlike products emerged when two equivalents of sodium acetate were added (see Figure S9c in the Supporting Information). Figure S10a in the Supporting Information shows that the product is composed of rhombic dodecahedrons and that the surface of the product is rough in the presence of 13.3 mL of ethanol and 6.7 mL of water. The crystal morphology changed from spheres to cubes and rods with increasing amounts of sodium acetate (see Figure S10b–d in the Supporting Information). Interestingly, cubes with truncated edges of about 1 μm were observed in 20 mL of ethanol in the absence of water (Figure 6a). Ligand H_3BTB is soluble in ethanol and has poor solubility in water; herein, we propose that the higher solubility of H_3BTB in ethanol benefits the formation of MOF-14 crystal-growth units and increases the supersaturation. Therefore, cubes with truncated edges with high-energy surfaces were obtained. Remarkably, individual spherelike and cubelike superstructures in the range of 1–2 μm were obtained when 1–2 equivalents of sodium acetate with respect to H_3BTB were added, and the superstructures were accumulated by numerous cubic units (Figure 6b, c). Particles of about 50 nm were observed when more sodium acetate was added (Figure 6d). According to such results, the particle morphology and size are crucially affected by the volume ratio of ethanol and water and the acid/base environment of the reaction system.

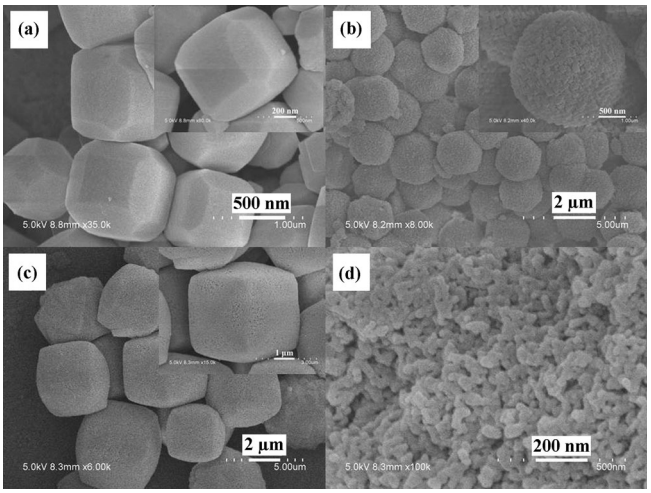

Figure 6. SEM images and high-magnification SEM images (inset) of MOF-14 microcrystals prepared in ethanol with different amounts of sodium acetate: a) 0, b) 1, c) 2, and d) 3 equivalents.

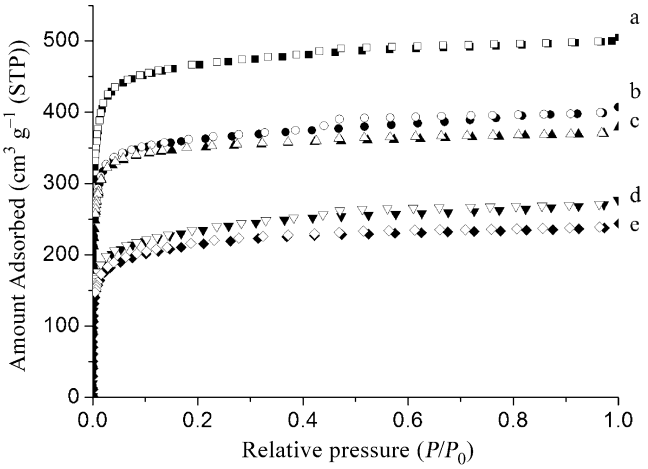

Figure 7. Adsorption and desorption isotherms of nitrogen (at 77 K) for MOF-14 microcrystals prepared with different amounts of sodium acetate: a) 0, b) 1, c) 2, d) 3, and e) 4 equivalents (solid and open markers represent adsorption and desorption, respectively).

In an effort to explore potential applications and the morphology-dependent property of the polyhedral microcrystals, gas-adsorption measurements were conducted on the MOF-14 microcrystals with different shapes prepared in the mixed solvent of ethanol and water (20 mL, 4:1 v/v). All the evacuated samples show a characteristic type I sorption isotherm (Figure 7), which is typical for microporous materials with a high level of N_2 adsorption at 77 K. The BET and Langmuir surface areas of the samples prepared with different amount of sodium acetate (see Table S1 in the Supporting Information), thus implying that the sample prepared without sodium acetate has the highest BET surface area of 1841 $m^2 g^{-1}$ and Langmuir surface area of 2155 $m^2 g^{-1}$, which is much higher than the reported value of 1502 $m^2 g^{-1}$ (Langmuir surface area) and indicates an excellent specific surface area of microporous MOF-14 crystals.[21] Increasing the amount of sodium acetate

decreases the Langmuir surface area from 1617, 1561 to 1054, 967 $m^2 g^{-1}$, (see Table S1 in the Supporting Information) thus indicating that the presence of sodium acetate has a significant effect on the gas-adsorption property and decreases the Langmuir surface. The crystal morphology of exposed surfaces has been reported as an important factor that could affect the gas-sorption property of MOF microcrystals.[10c,d,26] In the case of MOF-14, two exposed crystal facets {100} and {110} were determined by the different amounts of base and revealed two porous channels with inconsistent orientations on the crystal surfaces of the MOF-14 structure, which may lead to a differentiation in N_2 uptake. Meanwhile, the lowest sorption amount of the cubic crystals may also be attributed to the lowest crystallinity and growth defects caused by the fastest rate of the formation of the particles, which may block the channels. On the basis of the above results, the surface area decreases with increasing amounts of added sodium acetate, and MOF-14 microcrystals with different shapes lead to different gas-adsorption properties.

The adsorption and desorption of N_2 and CO_2 at 273 K were also performed for the MOF-14 microcrystals with different morphologies (see Figures S11–S15 in the Supporting Information for the results). All the samples show remarkable CO_2 uptake at 273 K and 1 bar, whereas little N_2 adsorption was observed, thus indicating excellent adsorption selectivity for CO_2 over N_2 for MOF-14 microcrystals. The adsorption amount of CO_2 for MOF-14 at 273 K and 1 bar decreases with the morphological evolution from rhombic dodecahedron to cube, which agrees well with the specific surface area; however, the estimated adsorption selectivity for CO_2 over N_2 increases accordingly (see Table S1 in the Supporting Information).

Conclusion

We have demonstrated a general approach toward the facile synthesis of porous coordination-polymer MOF-14 microcrystals with controlled morphologies and sizes by tuning the acid/base environment of the reaction system at room temperature. Sodium acetate not only leads to a morphological evolution of MOF-14 microcrystals from rhombic dodecahedron to truncated rhombic dodecahedron, cube with truncated edges, and finally to cube, but also decreases the particle size by accelerating the nucleation rate of the particles. This simple synthetic method avoids the use of high pressure, heat, and harmful solvents such as DMF; furthermore, this approach results in the formation of framework structures with well-defined morphologies, high crystallinities, and excellent gas-adsorption properties. The applicability of this method was demonstrated for the synthesis of HKUST-1, and the crystal morphologies and sizes were also determined by the acid/base environment of the reaction system. The gas-adsorption property of the MOF-14 microcrystals was dependent on the morphology of the particles.

Experimental Section

Preparation of MOF-14

All the commercially available chemicals and solvents were of reagent grade and were used as received without further purification. Ligand H_3BTB was synthesized according to a reported method.[27] In a typical experiment, H_3BTB (22 mg, 0.05 mmol) was dissolved in ethanol (16 mL) and deionized water (4 mL) under ultrasonic wave conditions. Sodium acetate (0–5 equiv with respect to H_3BTB) or other additives was added to this solution under stirring to give a clear solution. $Cu(NO_3)_2{\cdot}3H_2O$ (24 mg, 0.1 mmol) was added to the reaction mixture with stirring at ambient temperature. The mixed solution was stirred for 30 min at room temperature, and blue precipitates were subsequently collected by centrifugation, washed with distilled water and absolute ethanol several times, and dried under vacuum at 60 °C for 5 h (see the experimental details in the Supporting Information).

Preparation of HKUST-1

In a typical experiment, H_3BTC (4.2 mg, 0.02 mmol) was added to ethanol (25 mL) and deionized water (25 mL) under ultrasonic wave conditions. Different equivalents of bases (sodium acetate, aqueous ammonia, or NaOH) with respect to H_3BTC were added with stirring to this solution to give clear solution. $Cu(NO_3)_2{\cdot}3H_2O$ in aqueous solution (0.3 mL, 0.1 M) was added to the reaction mixture with stirring at room temperature. After 30 min, blue precipitates were subsequently collected by centrifugation, washed with distilled water and absolute ethanol several times, and dried under vacuum at 60 °C for 5 h.

Characterization

The PXRD data of the products were collected on a Bruker D8 Advance X-ray diffractometer with CuKα ($\lambda = 1.5418$ Å) radiation at room temperature. SEM observations were performed on a Hitachi S-4800 field emission scanning electron microscope at an accelerating voltage of 5 kV. TGA was performed on a Mettler-Toledo (TGA/DSC1) thermal analyzer in the temperature range 30–800 °C in a nitrogen atmosphere with a heating rate of 10 °C min^{-1}. FTIR spectra were recorded on a Bruker Vector22 FTIR spectrophotometer in the range $\lambda = 400$–$4000\ cm^{-1}$ with KBr pellets. N_2 and CO_2 sorption experiments were carried out on a Belsorp-max volumetric gas-sorption instrument. Surface areas were determined by using the BET and Langmuir methods. The ratio of the initial slopes of the CO_2 and N_2 adsorption isotherms was applied to estimate the adsorption selectivity for CO_2 over N_2 according to a previous report.[28] Prior to the N_2 and CO_2 sorption measurements, the samples were activated under vacuum at 373 K for about 5 h.

Acknowledgements

This work was financially supported by the National Natural Science Foundation of China (Grant no. 21331002 and 91122001) and the National Basic Research Program of China (Grant no. 2010CB923303).

Keywords: crystal growth · metal–organic frameworks · nanostructures · shape evolution · sorption property

[1] a) D. Wang, Y. Li, *Adv. Mater.* **2011**, *23*, 1044 – 1060; b) M. Oezaslan, M. Heggen, P. Strasser, *J. Am. Chem. Soc.* **2012**, *134*, 514 – 524; c) S.-C. Shiu, J.-J. Chao, S.-C. Hung, C.-L. Yeh, C.-F. Lin, *Chem. Mater.* **2010**, *22*, 3108 – 3113.

[2] a) X. Huang, Z. Zhao, J. Fan, Y. Tan, N. Zheng, *J. Am. Chem. Soc.* **2011**, *133*, 4718 – 4721; b) X. Xie, Y. Li, Z.-Q. Liu, M. Haruta, W. Shen, *Nature* **2009**, *458*, 746 – 749; c) S. Liu, J. Yu, M. Jaroniec, *Chem. Mater.* **2011**, *23*, 4085 – 4093.

[3] a) L. Zhang, W. Niu, G. Xu, *Nano Today* **2012**, *7*, 586 – 605; b) M. Jin, H. Zhang, Z. Xie, Y. Xia, *Angew. Chem.* **2011**, *123*, 7996 – 8000; *Angew. Chem. Int. Ed.* **2011**, *50*, 7850 – 7854; c) N. Tian, Z.-Y. Zhou, S.-G. Sun, Y. Ding, Z. L. Wang, *Science* **2007**, *316*, 732 – 735.

[4] G. Férey, *Chem. Soc. Rev.* **2008**, *37*, 191 – 214.

[5] a) M. P. Suh, H. J. Park, T. K. Prasad, D. W. Lim, *Chem. Rev.* **2012**, *112*, 782 – 835; b) J.-R. Li, J. Sculley, H.-C. Zhou, *Chem. Rev.* **2012**, *112*, 869 – 932.

[6] a) P. Horcajada, R. Gref, T. Baati, P. K. Allan, G. Maurin, P. Couvreur, G. Férey, R. E. Morris, C. Serre, *Chem. Rev.* **2012**, *112*, 1232 – 1268; b) D. Cunha, M. B. Yahia, S. Hall, S. R. Miller, H. Chevreau, E. Elkaïm, G. Maurin, P. Horcajada, C. Serre, *Chem. Mater.* **2013**, *25*, 2767 – 2776.

[7] a) L. E. Kreno, K. Leong, O. K. Farha, M. Allendorf, R. P. Van Duyne, J. T. Hupp, *Chem. Rev.* **2012**, *112*, 1105 – 1125; b) B. Liu, *J. Mater. Chem.* **2012**, *22*, 10094 – 10101.

[8] a) D. Zacher, O. Shekhah, C. Wöll, R. A. Fischer, *Chem. Soc. Rev.* **2009**, *38*, 1418 – 1429; b) Y. Liu, Z. Ng, E. A. Khan, H.-K. Jeong, C.-B. Ching, Z. Lai, *Microporous Mesoporous Mater.* **2009**, *118*, 296 – 301.

[9] a) L. Ma, C. Abney, W. Lin, *Chem. Soc. Rev.* **2009**, *38*, 1248 – 1256; b) M. Yoon, R. Srirambalaji, K. Kim, *Chem. Rev.* **2012**, *112*, 1196 – 1231.

[10] a) A. M. Spokoyny, D. Kim, A. Sumrein, C. A. Mirkin, *Chem. Soc. Rev.* **2009**, *38*, 1218 – 1227; b) Z. Xin, J. Bai, Y. Pan, M. J. Zaworotko, *Chem. Eur. J.* **2010**, *16*, 13049 – 13052; c) H. J. Lee, W. Cho, S. Jung, M. Oh, *Adv. Mater.* **2009**, *21*, 674 – 677; d) C. Y. Lee, Y.-S. Bae, N. C. Jeong, O. K. Farha, A. A. Sarjeant, C. L. Stern, P. Nickias, R. Q. Snurr, J. T. Hupp, S. T. Nguyen, *J. Am. Chem. Soc.* **2011**, *133*, 5228 – 5231; e) C. Scherb, A. Schödel, T. Bein, *Angew. Chem.* **2008**, *120*, 5861 – 5863; *Angew. Chem. Int. Ed.* **2008**, *47*, 5777 – 5779.

[11] a) Q. Liu, L.-N. Jin, W.-Y. Sun, *Chem. Commun.* **2012**, *48*, 8814 – 8816; b) G. Majano, J. Pérez-Ramírez, *Adv. Mater.* **2013**, *25*, 1052 – 1057.

[12] P. Horcajada, T. Chalati, C. Serre, B. Gillet, C. Sebrie, T. Baati, J. F. Eubank, D. Heurtaux, P. Clayette, C. Kreuz, J.-S. Chang, Y. K. Hwang, V. Marsaud, P.-N. Bories, L. Cynober, S. Gil, G. Férey, P. Couvreur, R. Gref, *Nat. Mater.* **2010**, *9*, 172 – 178.

[13] a) S. Diring, S. Furukawa, Y. Takashima, T. Tsuruoka, S. Kitagawa, *Chem. Mater.* **2010**, *22*, 4531 – 4538; b) A. Umemura, S. Diring, S. Furukawa, H. Uehara, T. Tsuruoka, S. Kitagawa, *J. Am. Chem. Soc.* **2011**, *133*, 15506 – 15513.

[14] a) Q. Liu, L.-N. Jin, W.-Y. Sun, *CrystEngComm* **2013**, *15*, 8250 – 8254; b) L.-G. Qiu, Z.-Q. Li, Y. Wu, W. Wang, T. Xu, X. Jiang, *Chem. Commun.* **2008**, 3642 – 3644; c) R. Ameloot, L. Stappers, J. Fransaer, L. Alaerts, B. F. Sels, D. E. De Vos, *Chem. Mater.* **2009**, *21*, 2580 – 2582.

[15] S. Hermes, T. Witte, T. Hikov, D. Zacher, S. Bahnmuller, S. Langstein, K. Huber, R. A. Fischer, *J. Am. Chem. Soc.* **2007**, *129*, 5324 – 5325.

[16] W. Cho, H. J. Lee, M. Oh, *J. Am. Chem. Soc.* **2008**, *130*, 16943 – 16946.

[17] J. Cravillon, R. Nayuk, S. Springer, A. Feldhoff, K. Huber, M. Wiebcke, *Chem. Mater.* **2011**, *23*, 2130 – 2141.

[18] M. Pang, A. J. Cairns, Y. Liu, Y. Belmabkhout, H. C. Zeng, M. Eddaoudi, *J. Am. Chem. Soc.* **2012**, *134*, 13176 – 13179.

[19] T. Uemura, Y. Hoshion, S. Kitagawa, K. Yoshida, S. Isoda, *Chem. Mater.* **2006**, *18*, 992 – 995.

[20] H. Guo, Y. Zhu, S. Wang, S. Su, L. Zhou, H. Zhang, *Chem. Mater.* **2012**, *24*, 444 – 450.

[21] B. Chen, M. Eddaoudi, S. T. Hyde, M. O'Keeffe, O. M. Yaghi, *Science* **2001**, *291*, 1021 – 1023.

[22] a) J. R. Karra, B. E. Grabicka, Y.-G. Huang, K. S. Walton, *J. Colloid Interface Sci.* **2013**, *392*, 331 – 336; b) M. Klimakow, P. Klobes, A. F. Thünemann, K. Rademann, F. Emmerling, *Chem. Mater.* **2010**, *22*, 5216 – 5221.

[23] S. S.-Y. Chui, S. M.-F. Lo, J. P. H. Charmant, A. G. Orpen, I. D. Williams, *Science* **1999**, *283*, 1148 – 1150.

[24] H.-X. Lin, Z.-C. Lei, Z.-Y. Jiang, C.-P. Hou, D.-Y. Liu, M.-M. Xu, Z.-Q. Tian, Z.-X. Xie, *J. Am. Chem. Soc.* **2013**, *135*, 9311 – 9314.

[25] F. Wang, H. Guo, Y. Chai, Y. Li, C. Liu, *Microporous Mesoporous Mater.* **2013**, *173*, 181 – 188.

[26] M.-H. Pham, G.-T. Vuong, F.-G. Fontaine, T.-O. Do, *Cryst. Growth Des.* **2012**, *12*, 3091 – 3095.

[27] E. Weber, M. Hecher, E. Koepp, W. Orlia, *J. Chem. Soc. Perkin Trans. 2* **1988**, 1251 – 1257.

[28] J. An, S. J. Geib, N. L. Rosi, *J. Am. Chem. Soc.* **2010**, *132*, 38 – 39.

Received: April 2, 2014
Published online on September 15, 2014